J. Electrochem. Sci. Eng. **13(3)** (2023) 553-561; http://dx.doi.org/10.5599/jese.1660

Open Access : : ISSN 1847-9286
https://pub.iapchem.org/ojs/index.php/JESE

Original scientific paper

Performance of magnetized tool in electrochemical micromachining on scrapped alloy wheel matrix composite

Venugopal Palaniswamy[1,] ✉ and Thanigaivelan Rajasekaran[2]

[1]*Department of Mechanical Engineering, Muthayammal College of Engineering, Rasipuram 637408, India*

[2]*AKT Memorial College of Engineering and Technology, Kallakurichi, Tamil Nadu606 213, India*

Corresponding author: ✉ *tvelan10@gmail.com*

Received: January 7, 2023; Accepted: March 9, 2023; Published: March 13, 2023

Abstract

Hybrid machining processes play an important role in traditional and non-traditional machining processes. Adding the magnetic field effect in electrochemical micromachining (ECMM) improves the machining efficiency and accuracy of the micro-hole machined. The process parameters, namely, voltage, duty cycle and electrolyte concentration were used as input parameters, while machining rate (MR) and overcut (OC) are performance measures considered in this research. The workpiece was a scrapped alloy wheel matrix fabricated with a stir-casting process reinforced with alumina (Al_2O_3). The EDAX and SEM image study was performed to understand the composition and surface quality of the machined workpiece, respectively. The micro-hole without magnetic field effect was also conducted to understand the possible advantage of the magnetic field applied in ECMM.

Keywords

Aluminum metal matrix composite; magnetic field; machining rate (MR); machining overcut (OC)

Introduction

The industrial usage of aluminum metal matrix composites (Al-MMCs) is increasing day by day due to their unique properties compared to alloy materials. Al-MMCs have several advantageous properties, such as a high strength-/stiffness-to-weight ratio, high resistance to fatigue, excellent wear, corrosion, and temperature resistance. Al-MMCs are widely used in the aerospace, defense, and automotive industries, where they must be machined to the correct size and shape. The hybrid MMC is more difficult to machine than traditional materials, primarily because of the increased hardness and strength provided by the reinforced particles. In such a case, electrochemical machining (ECM), working with tool and workpiece electrodes, electrolyte and voltage supply, could be efficiently applied [1,2].

Ao *et al.* [1] have considered a new-generation ECM process for machining SiC particle-reinforced Al-MMCs. The study revealed that a higher voltage supports a large depth in a workpiece. The surface roughness relies on electrolyte choice and voltage type and level. Ibrahim *et al*. [2] have machined Al-MMCs through electrochemical micromachining (ECMM) and optimized ECMM parameters. The optimized combination for radial overcut (OC) was 10 g l^{-1} of electrolyte concentration, voltage of 10 V, and inter-electrode gap of 0.3 mm. Also, the electrolyte concentration of 30 g l^{-1}, voltage of 18 V, and inter-electrode gap of 0.2 mm were found as the optimal parametric combination for the material removal rate (MRR). Prakash *et al*. [3] have varied voltage, electrolyte concentration, duty cycle, and tool feed rate to optimize MR, radial OC, surface roughness and wear on tool electrode. The obtained results coincide with the response surface method result for a surface roughness value of 0.4 µm. Kunar *et al*. [4] have reused a textured tool in ECMM and documented that the electrolyte concentration of 10 g l^{-1}, pulsed frequency of 190 kHz produces high quality micro circular pattern with higher machining accuracy. Arul *et al*. [5] have used an Al-MMC electrode to machine copper workpiece and found that the Al-MMC electrode can be used for producing lesser OC holes. Maniraj *et al*. [6] have developed a furnace slag-reinforced Al-MMC sand machine using ECMM and studied the effect of process parameters on machinging rate (MR) and OC. L_{18} mixed-level orthogonal array was used for executing the experiments. It was found that the composition of ground granulated blast furnace slag (GGBS) plays a major role in affecting the machining performance. In another paper, Maniraj *et al*. [7] studied the ECMM performance with a heated electrode on MR, conicity factor (CF) and OC. They reported that the heated electrode improves the MR by 88.37 %, reduces the OC by 37.03 % and reduces the CF by 33.33 % compared to the ordinary electrode. Generally, machinability studies using ECMM on metal matrix composites are sparse. Moreover, the use of a magnetized tool in ECMM on scrapped alloy wheel matrix composites is of the first kind [8-13].

In this research, the ECMM input parameters are varied and the effect of magnetized tool electrode on MR and OC is studied. Moreover, the composition of the casted Al-MMC is studied using EDAX and surface quality studies are performed using the SEM technique.

Experimental

Figure 1 shows the experimental setup used for the ECMM process. The setup consisted of a pulsed power supply unit and machine structure.

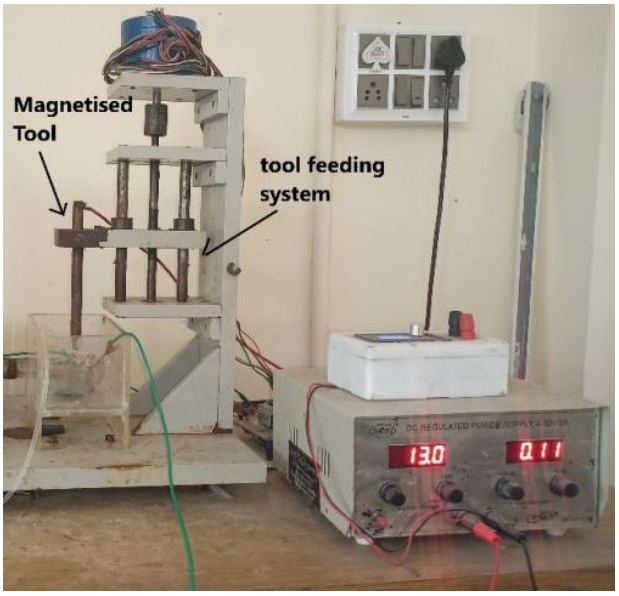

Figure 1. *ECMM machine*

The machine structure consists of 3 angle plates and one vertical plate. The stepper motor is housed on one angle and the remaining two angle plates support the tool feeding arrangement. The tool-feeding arrangement consists of a sliding rod and lead screw. The tool holder will slide up and down in the sliding rod powered by a stepper motor. The stepper motor is programmed to rotate at 6° per pulse. The electrode gap is the gap between the tool electrode face and the workpiece surface, which is controlled by stepper motor movement. The tool electrode holder is made up of copper material and a negative power supply is provided to the tool through the tool holder. The commercially available ten numbers of hollow N 52 grade permanent neodymium magnets were used for producing the magnetic flux. These magnets are attached to the tool holder, as depicted in Figure 2.

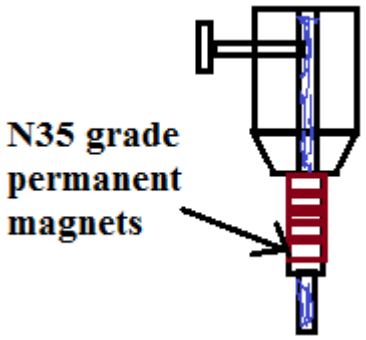

Figure 2. *Sketch of permanent magnet with the tool*

The stainless-steel electrode of diameter 480 µm is used as the tool electrode. The chemical composition of the electrode is 58.80 % nickel, 12.32 % tungsten, and 11.19 % aluminum with chromium, iron and cobalt [14].The electrode is coated with epoxy to prevent stray current effects [15]. The electrolyte was prepared using sodium nitrate ($NaNO_3$) salt mixed with distilled water. Different concentrations of $NaNO_3$ brine solution are prepared (15-35 g l^{-1}) and used for experiments. The electrolyte is circulated to the machining through a pump and filter arrangement. The debris produced during the machining process was filtered using micro-level filters. The workpiece was prepared using the scrapped alloy wheel and aluminum oxide. Honda car scrapped wheels of the chemical compositions copper, silicon, iron, zinc, tin, lead, titanium and aluminum of 0.09, 11.13, 2.92, 0.06, 0.19, 0.29, 1.70 and 83.62 wt.%, respectively, were used as a base metal. The scrapped alloy wheel was melted in a stir-casting setup and aluminum oxide was used as reinforcement. The developed Al-MMC was cut into sheets having a thickness of 300 µm for ECMM. The content of the elements listed in Table 1 shows the quantitative composition of the workpiece. Comparing the composition of casted workpiece and scrapped alloy wheel, it appears that in the casted workpiece, aluminum is reduced to 30.36 wt.%, while oxygen is newly present with 13.87 wt.%.

Table 1. *Composition of the workpiece*

Element	Content, wt %	Content, at.%	Error, %
C	8.51	16.61	16.33
O	13.87	20.33	9.59
Na	1.54	1.57	10.9
Mg	5.00	4.83	5.92
Al	30.36	26.37	4.42
Si	31.88	26.61	5.85
S	0.04	0.03	18.12
Cr	0.85	0.38	14.54
Fe	4.64	1.95	5.11
Ni	3.30	1.32	7.27

The electrochemical cell is formed by stainless steel and workpiece electrodes submerged in the electrolyte solution. By applying a voltage difference between the stainless steel electrode (cathode) and workpiece (anode), the electrolysis process is ensured. During the electrolysis process, metal ions from Al-MMC workpiece anode dissolve and move towards the bulk electrolyte and the stainless-steel cathode. At the same time, negative ions from the electrolyte are attracted by the workpiece anode. The hydrogen gas bubbles are released at the cathode by water breakdown during electrolysis. Produced OH^- ions combine with metal ions and form insoluble metal hydroxides, precipitating and removing metal ions from the system. The formation of metal hydroxides is a chemical process occurring out of electrodes and does not affect the total current flowing between electrodes.

For experiments, the input variables, namely voltage, electrolyte concentration and duty cycle along with permanent magnet field effect, are investigated on MR and OC. During machining, the frequency was kept constant at 50 Hz. The total time was calculated from the frequency of 50 Hz, equal to 20 milliseconds, and the duty cycle is the ratio of pulse on time to the total time.

Table 2 shows the experiment parameters and output performance. During the machining process, the time taken for machining a through hole is noted in seconds.

Table 2. *Experiment levels and output performance*

S.No	Voltage, V	Duty cycle, %	Electrolyte concentration, g l^{-1}	MR, µms^{-1}	OC, µm
1	6	90	35	0.1111	800
2	7	90	35	0.1190	840
3	8	90	35	0.1315	900
4	9	90	35	0.1562	940
5	10	90	35	0.2500	970
6	10	50	35	0.1041	820
7	10	60	35	0.1282	860
8	10	70	35	0.1111	910
9	10	80	35	0.1851	950
10	10	90	35	0.2380	990
11	10	90	15	0.1428	870
12	10	90	20	0.1562	890
13	10	90	25	0.1785	910
14	10	90	30	0.2000	930
15	10	90	35	0.2777	940

The thickness of the workpiece sheet was measured using a micrometer and recorded in µm. The MR is calculated by dividing the thickness of the workpiece sheet by the machining time. The OC is calculated by finding the difference between a tool and a machined hole diameter. The electrode diameter is measured in µm using a micrometer and the machined hole diameter is using the optical microscope image data.

Results and discussion

Effect of voltage along with magnetic field on MR and OC

Figure 3 shows the effect of voltage and magnetic field on the machining rate and MR and OC. It is obvious from Figure 4 that MR and OR increase with the voltage increase. The MR increases firstly slowly from 6 to 8 V and then steeply from 8 to 9 V. The drastic increase in the MR is observed from 9 to 10 V. The increase in voltage enhances the current density required for machining, which is attributed to the increasing trend of MR. Introducing a magnet creates a Lorentz force, a mixture of

electric and magnetic force, which act on charged particles. The arrangement of a magnet on the tool electrode induces a Lorentz force, resulting in increased mobility of ions and improved dissolutions process. In ECMM, the material removal takes place due to the dissolution of ions from the anode and with the aided magnetic force, the MR increases. The drastic increase in MR for higher voltage is due to the fact that at a higher voltage level, the current density required for machining is higher and along with Lorentz force, higher MR is observed. As seen in Figure 3, OC tends to increase with the voltage but in a weaker manner than MR. During ECMM, the removal of dissolute from the electrolyte is necessary for efficient machining. Normally in ECMM, the OC produced is three times the electrode diameter and OC observed in Al-MMCs is higher compared to alloys [8-10]. The OC of the micro-hole mainly depends on the current density, improper evacuation of debris, bridging of the electrode by debris and inadequate tool tip insulation. The presence of the magnetic field effect lines up the debris and dispels it from the machining zone, which can be attributed to lesser OC. Figure 4 shows the micro-hole machined using the magnetic field effect with less delaminated areas and circularity.

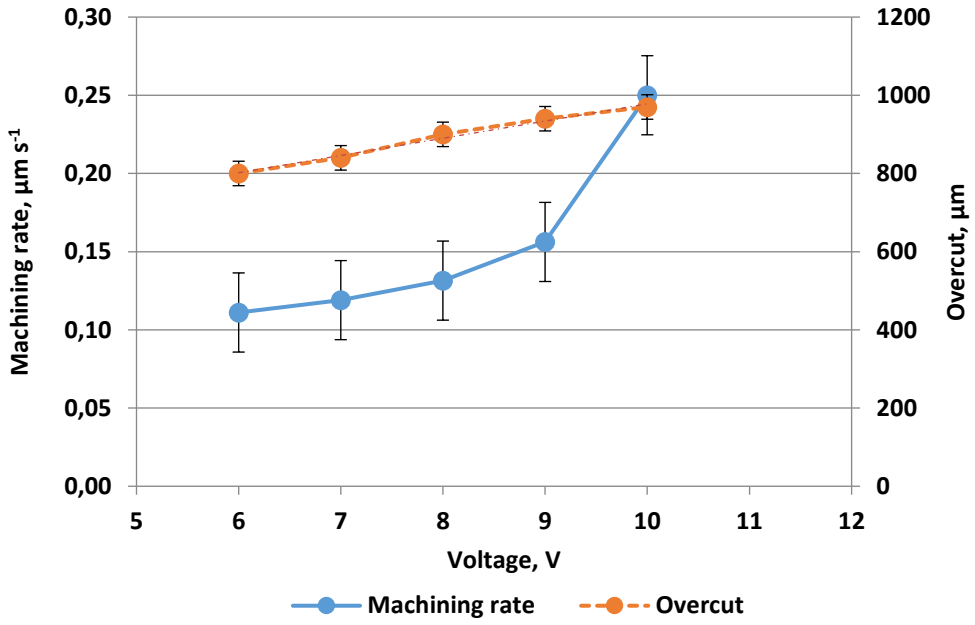

Figure 3. *MR and OC vs.voltage*

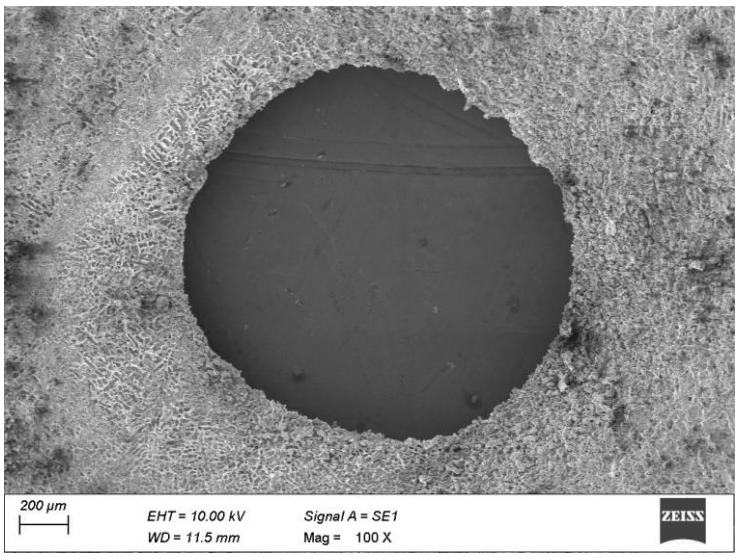

Figure 4. *Micro-hole on Al-MMCwith magnetic effect*

Effect of duty cycle with magnetic effect on MR and OC

Figure 5 shows the effect of the duty cycle on MR and OC. An increase in the duty cycle increases the MR since an increase in the duty cycle enhances the pulse on the current required for machining. The long-duration availability of pulse on current can be attributed to higher MR. For the duty cycle of 50 to 70 %, the increasing and decreasing trend in MR is observed. The MR increases significantly for higher duty cycles (70 to 90 %), which is caused by the fact that the current density is higher at higher duty cycles. This phenomenon increases the MR along with the magnetic field effect. The rate of change of OC is more with the duty cycle and the presence of a magnetic field reduces the OC irrespective of faster dissolution due to the prolonged pulse time on time. Figure 6 shows the micro-hole with lesser OC, micro cracks and delaminated surfaces.

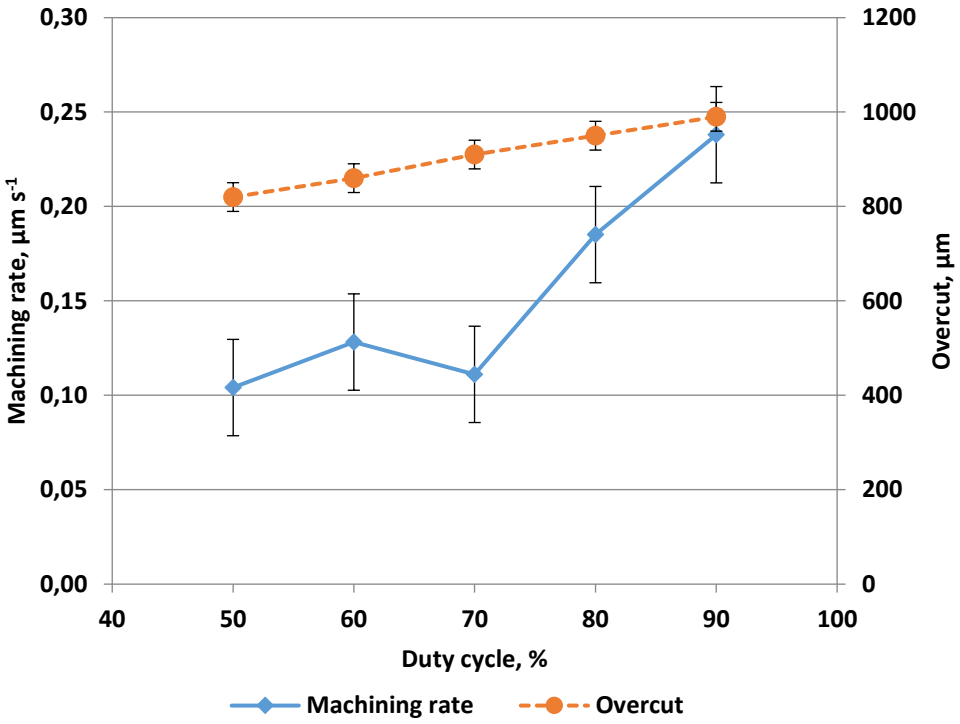

Figure 5. *Effect of duty cycle on MR and OC*

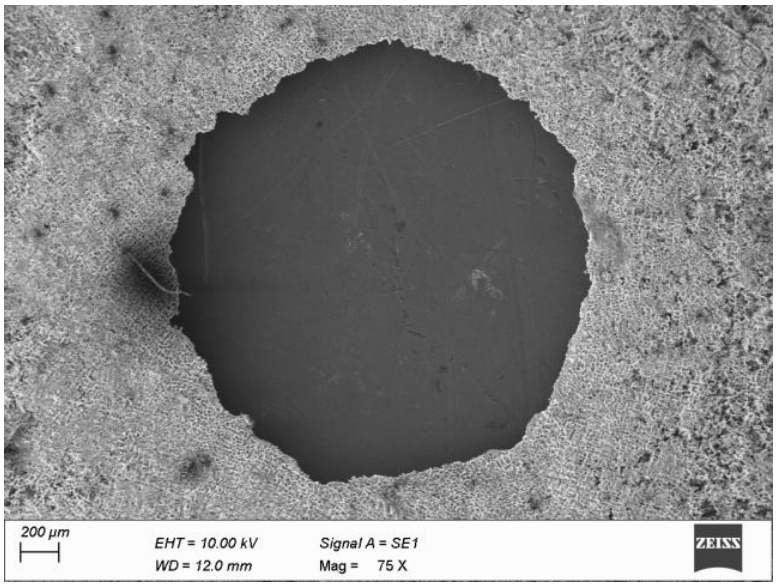

Figure 6. *Microhole machined at 10 V, 90 % and 35 g l^{-1}*

Effect of electrolyte concentration on MR and OC

MR and OR increase with an increase of electrolyte concentration, which is evident from Figure 7. The rate of change in MR is less for concentrations up to 30 g l^{-1}, and then increases drastically for higher electrolyte concentrations. At higher electrolyte concentrations, more ions are available for machining, and the presence of Lorentz force accelerates the machining performance. The presence of Lorentz force induces magneto-hydrodynamic convection in the electrolyte.

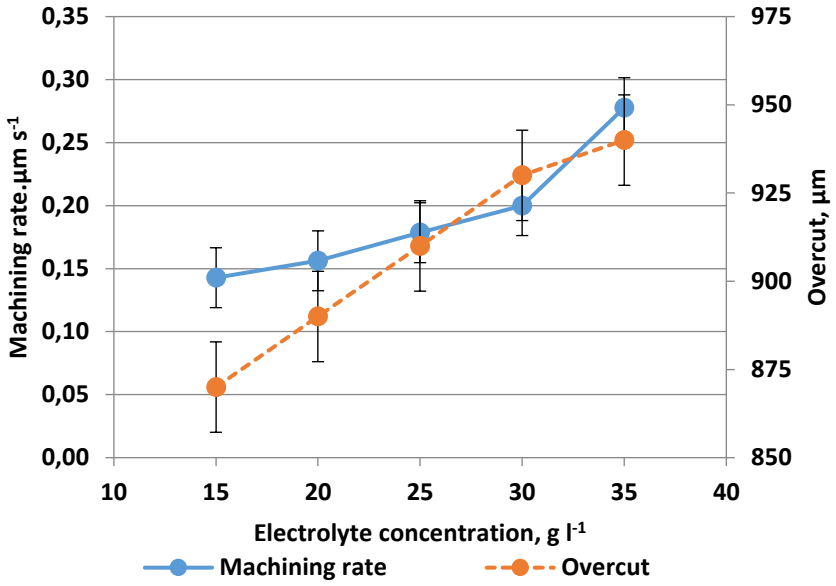

Figure 7. *MR and OC vs. electrolyte concentration*

This phenomenon slightly increases the temperature of the electrolyte and electrolyte circulation in the machining zone. Moreover, the presence of a magnetic field alters the trajectory motion of charged ions. This motion of ions induces the stirring effect in the electrolyte. With ethe ffect of the magnetic field, the charged ions will move along spiral lines and more ions reach the machining zone, as shown in Figure 8 [11]. Higher growth of MR is observed for the electrolyte concentration of 30 to 35 g l^{-1}. The rate of change of OC, however, is high for the electrolyte concentration of 15 to 30 g l^{-1}. Although the increase in electrolyte concentration results in much debris due to a higher dissolution rate, the presence of a magnetic field effect orients the debris away from the machining zone [12,13]. Figure 9 shows the micro-hole machined on Al-MMCs with lesser micro-cracks and stray current affected zone. Few pores are witnessed due to the detachment of micro reinforcement particles during the dissolution process. Figure 10 shows the micro-hole machined without a magnet and more debris attachment; delaminated surfaces and micro pits are observed on the micro-hole's circumference.

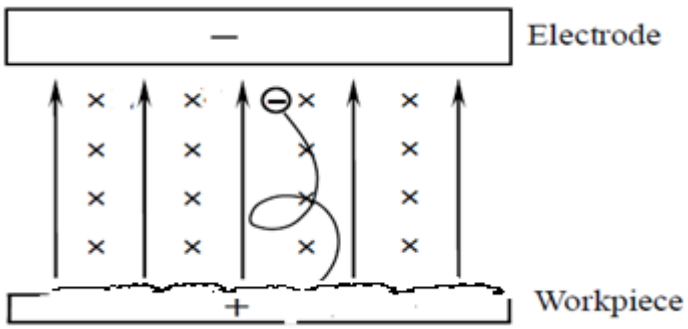

Figure 8. *Sketch of ion movement in magnetic field [11]*

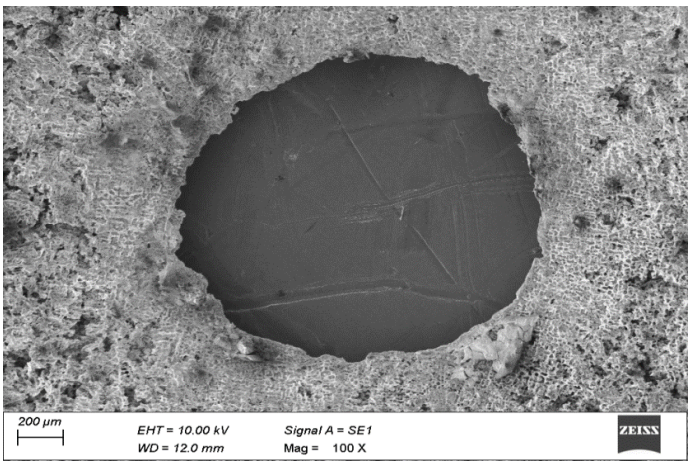

Figure 9. *Micro-hole machined at 10 V, 90 % and 25 g* l^{-1}

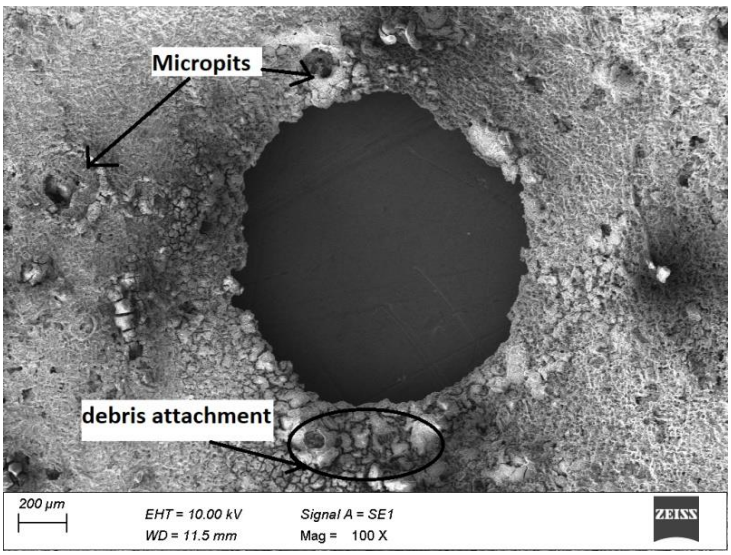

Figure 10. *Micro-hole machined without magnet field at 10 V, 90 % and 25 g* l^{-1}

Conclusions

The scrapped alloy wheel matrix with Al_2O_3 reinforcement is produced and tested for the presence of elements. The ECMM experiments were planned using varying one parameter at a time with a permanent magnetic field effect. The MR increased rapidly for voltage levels of 9 to 10 V, while less rate of change of OC is observed for the voltage range of 6 to 10 V. Duty cycle range of 70 to 90 %, along with the magnetic field effect, shows higher MR and high rate of change of OC. The electrolyte concentration of 30 to 35 g l^{-1} produces higher MR, while a high rate of change of OC is observed for the electrolyte concentration range of 15 to 30 g l^{-1}. Moreover, the micro-hole produced has lesser OC, delaminated area, stray current affected zone, micro cracks and micro-pits. The micro-hole machined without a magnetic field resulted in more debris attachment on the circumference of the micro-hole.

References

[1] S. Ao, X. Qin,K. Li, Z. Luo, Effects of process parameters on jet electrochemical machining of SiC particle-reinforced aluminum matrix composites, *The International Journal of Advanced Manufacturing Technology* **112(11)** (2021) 3351-3361. https://doi.org/10.1007/s00170-020-06586-y

[2] A. F. Ibrahim, S. M. Mousa, D. A. al Kareem Noori, Investigation and optimization of machining parameters in electrochemical machining of aluminium metal matrix composites,

Periodicals of Engineering and Natural Sciences **10(3)** (2022) 48-59. http://dx.doi.org/10.21533/pen.v10i3.3006

[3] J. Prakash, S. Gopalakannan, Teaching—learning-based optimization coupled with response surface methodology for micro electrochemical machining of aluminium nano composite, *Silicon* **13(2)** (2021) 409-432. https://doi.org/10.1007/s12633-020-00434-0

[4] S. Kunar, A. P. Tiwary, G. Kibria, B. V. Prasad, Investigation into Machining Accuracy of Micro Circular Pattern Fabricated by Maskless Electrochemical Micromachining, *The Journal of Engineering Science and TechnologyReview* **14(4)** (2021) 99-104.

[5] A. T. Ganesan, P. Varthajaru, T. Rajasekaran, Performance Study of Electrochemical Micromachining Using Square Composite Electrode for Copper, *Chemical Industry & Chemical Engineering Quarterly* **28(3)** (2022) 247-253. https://doi.org/10.2298/CICEQ210501036A

[6] S. Maniraj, R. Thanigaivelan, Optimization of Electrochemical Micromachining Process Parameters for Machining of AMCs with Different % Compositions of GGBS Using Taguchi and TOPSIS Methods, *Transactions of the Indian Institute of Metals* **72** (2019) 3057-3066. https://doi.org/10.1007/s12666-019-01772-3

[7] S. Maniraj, R. Thanigaivelan, Effect of electrode heating on performance of electrochemical micromachining, *Materials and Manufacturing Processes***34(13)**(2019) 1494-1501. https://doi.org/10.1080/10426914.2019.1655153

[8] J. R. Vinod Kumaar, R. Thanigaivelan, Performance of magnetic field-assisted citric acid electrolyte on electrochemical micro-machining of SS 316L, *Materials and Manufacturing Processes* **35(9)** (2020) 969-977. https://doi.org/10.1080/10426914.2020.1750630

[9] R. Thanigaivelan, R. M. Arunachalam, Experimental study of overcut in electrochemical micromachining for 304 stainless steel, 38th North American Manufacturing Research Conference 2010 (NAMRI/SME NAMRC 38), Kingston, Ontario, Canada, *Transactions of NAMRI/SME* **38** (2010) 253-260. ISBN 9781617389399

[10] S. Maniraj, R. Thanigaivelan, R. Viswanathan, P. Elumalai, Experimental investigation of MRR and ROC in aluminium metal matrix composites, *Materials Today: Proceedings* **45** (2021) 1102-1106. https://doi.org/10.1016/j.matpr.2020.03.190

[11] C. Zhang, P. Zheng, R. Liang, K. Yun,X. Jiang, Z. Yan, Effects of a magnetic field on the machining accuracy for the electrochemical drilling of micro holes, *International Journal of Electrochemical Science* **15** (2020) 1148-1159.https://doi.org/10.20964/2020.02.10

[12] T. Weier, J.Hüller, G. Gerbeth, F.-P. Weiss, Lorentz force influence on momentum and mass transfer in natural convection copper electrolysis, *Chemical Engineering Science* **60(1)** (2005) 293-298. https://doi.org/10.1016/j.ces.2004.07.060

[13] S. Kumar, M. Goud, N. M. Suri, Experimental investigation of magnetic-field-assisted electric discharge machining by silicon-based dielectric of Inconel 706 superalloy, *Sādhanā* **45(1)** (2020) 253. https://doi.org/10.1007/s12046-020-01493-0

[14] P. Venugopal, T. G. Arul, R. Thanigaivelan, Performance optimization of a PTFE-coated electrode in electrochemical micromachining, *Ionics* **28** (2022) 4745-4753. https://doi.org/10.1007/s11581-022-04686-1

[15] V. Palaniswamy, K. Seeniappan, T. Rajasekaran, N. Lakshmaiya, Enhancing MRR and accuracy with magnetized graphite tool in electrochemical micromachining of copper, *Chemical Industry & Chemical Engineering Quarterly* **29(3)** (2023) 201-208. https://doi.org/10.2298/CICEQ220731027P